INTERNATIONAL JOURNAL FOR NUMERICAL METHODS IN FLUIDS, VOL. 3, 61–70 (1983)

EVALUATION OF TIDAL RESIDUAL CURRENTS IN A WIDE ESTUARY, USING A FINITE ELEMENT METHOD

A. D. JENKINS

Department of Offshore Engineering, Heriot-Watt University, Riccarton, Currie, Edinburgh EH14 4AS, Scotland

SUMMARY

From the linearized, time-independent, constant depth, shallow water tidal equations in an f-plane for a two-layer estuary, two independent modal Helmholtz equations are derived. These modal equations are solved using a fifth-degree finite element technique. The first and second space derivatives of the complex modal tidal elevations, and thus the modal currents and their first derivatives, are evaluated directly from the solution at each node of the finite element mesh.

The Stokes drift, which is the major part of the residual tidal flow, is evaluated from these nodal values of the currents and their derivatives. Good agreement is obtained with the exact analytical solution for a wedge-shaped estuary with a wedge angle of $\pi/3$, using a mesh of 64 equilateral triangles with sides approximately $\frac{1}{10}$ of the wavelength $2\pi c_2/\sigma$ of a Kelvin wave solution for the short-wavelength mode.

KEY WORDS Tides Residual Currents Finite Elements Modal Separation

1. INTRODUCTION

When suspended or floating material is moved by currents it is the Lagrangian mean or residual currents which will determine how far in which direction such material will travel. These residual currents can be due to any combination of the three physical mechanisms of tides, density differences and wind—this paper develops a model of the residual current caused by a combination of tides and density differences.

For a velocity field $\mathbf{u}(\mathbf{x}, t)$ varying periodically with time, where the excursion of a fluid particle during one period of oscillation is small compared to the length scale of the velocity field, the Lagrangian mean velocity or mass transport velocity $\mathbf{u}_L$ is given by[1]

$$\mathbf{u}_L = \bar{\mathbf{u}} + \overline{\int_{t_0}^{t} \mathbf{u}\, dt' \cdot \nabla \mathbf{u}} \tag{1}$$

where the overbar denotes the average over a complete period. $\bar{\mathbf{u}}$ is the *Eulerian residual* velocity which, for conditions appropriate to tidal flow, Dyke[2] found to be an order of magnitude less than the Stokes drift

$$\overline{\int_{t_0}^{t} \mathbf{u}\, dt' \cdot \nabla \mathbf{u}}$$

However, friction and non-linear effects cannot in general be neglected in tidal flows, and under such circumstances the oscillation of $\mathbf{u}(\mathbf{x})$ becomes unsymmetrical, increasing the Eulerian residual $\bar{\mathbf{u}}$. Nevertheless, field measurements[3] have shown significant differences between $\mathbf{u}_L$ and $\bar{\mathbf{u}}$, which are probably attributable to Stokes drift.

0271–2091/83/010061–10$01.00

Received 14 December 1981
Revised 23 March 1982

Dyke[4] showed that, whereas the residual flow is small in a homogeneous estuary, if there are two (or more) layers of different density, there is a much larger residual flow in each layer (in different directions). The method of modal separation which he used is reproduced in the next section with slight changes in notation.

2. THE TIDAL EQUATIONS AND THEIR ANALYTICAL SOLUTION

The following equations[4,5] describe linear two-dimensional tidal motions in a two-layer sea.

$$\frac{\partial \mathbf{u}'}{\partial t} + \mathbf{f} \times \mathbf{u}' + g\nabla\zeta' = \mathbf{0} \tag{2}$$

$$\frac{\partial}{\partial t}(\zeta' - \zeta'') + h'\nabla \cdot \mathbf{u}' = 0 \tag{3}$$

$$\frac{\partial \mathbf{u}''}{\partial t} + \mathbf{f} \times \mathbf{u}'' + g\nabla((1+\alpha)\zeta' + \alpha\zeta'') = \mathbf{0} \tag{4}$$

and

$$\frac{\partial \zeta''}{\partial t} + h''\nabla \cdot \mathbf{u}'' = 0 \tag{5}$$

In these equations, g is the acceleration due to gravity, h is the equilibrium total depth ($=h'+h''$), h' and h'' are the equilibrium thicknesses of the upper and lower layers, respectively, ζ' and ζ'' are the departures of the levels of the sea surface and the interface from equilibrium. $\mathbf{u}'$ and $\mathbf{u}''$ are the horizontal fluid velocities in the layers. $\alpha = (\rho'' - \rho')/\rho''$ is the fractional density difference between the two layers. $\mathbf{f}$ is a vector directed vertically upwards, with magnitude f equal to the Coriolis parameter, which is assumed constant (f-plane approximation). Rattray showed that (2)–(5) can be split into two independent modes if the following substitutions are made, to lowest order in α:

$$\mathbf{u}_1 = \frac{1}{h}(h'\mathbf{u}' + h''\mathbf{u}'') \tag{6}$$

$$\mathbf{u}_2 = \mathbf{u}' - \mathbf{u}'' \tag{7}$$

$$\zeta_1 = \zeta' \tag{8}$$

and

$$\zeta_2 = \alpha\left(\frac{h''}{h}\zeta' - \zeta''\right) \tag{9}$$

Mode 1 (the barotropic mode) represents the depth averaged motion of the water body: ζ_1 is the surface water elevation and $\mathbf{u}_1$ is the mean horizontal current. Mode 2 (the baroclinic mode) represents the depth variation of the current and the movement of the interface between the top and bottom layers. $\mathbf{u}_2$ is the change in current across the interface, and ζ_2 is proportional to the difference between the level of the interface and the level the interface would have had were the baroclinic mode absent.

For any one harmonic tidal constituent (say M_2), both modes will by definition have the same period. As we shall see below, the wavelength of the baroclinic mode will be much smaller than that of the barotropic mode, and the Coriolis effect will become important at correspondingly smaller scales.

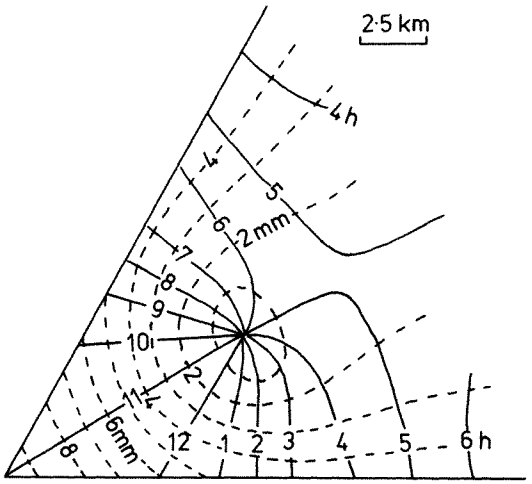

Figure 1. Cotidal and co-range lines for the interfacial mode 2 (mode 1 varies very slowly)

If we substitute

$$\zeta_m = \mathrm{Re}\,(Z_m \exp i\sigma t) \qquad (m = 1, 2), \tag{10}$$

and

$$\mathbf{u}_m = \mathrm{Re}\,(\mathbf{U}_m \exp i\sigma t) \tag{11}$$

where σ is the tidal angular frequency, we obtain the Helmholtz equations for both models, subject to appropriate boundary conditions, which are discussed below:

$$\nabla^2 Z_m + k_m^2 Z_m = 0 \qquad (m = 1, 2) \tag{12}$$

where

$$k_m = (\sigma^2 - f^2)^{1/2}/c_m$$
$$c_m = \sqrt{(gh_m)}$$

with $h_1 = h$ and $h_2 = \alpha h' h''/h$.

The boundary conditions for (12) are $Z_m = \bar{Z}_m$ on the open parts of $\partial_1 A$ of the boundary, and $\mathbf{U}_m \cdot \mathbf{n} = 0$ on the coastal parts $\partial_2 A$ of the boundary, where $\mathbf{n}$ is a vector normal to the coast. The $\mathbf{U}_m$ are determined by

$$\mathbf{U}_m = \frac{g}{\sigma^2 - f^2}(i\sigma \nabla Z_m - \mathbf{f} \times \nabla Z_m) \tag{13}$$

and hence, in terms of elevation derivatives, the coastal boundary condition becomes

$$i\sigma \frac{\partial Z_m}{\partial n} + f \frac{\partial Z_m}{\partial s} = 0$$

where n is the outward normal and s is directed anticlockwise around the boundary.

In the upper layer the Stokes drift is given by

$$\mathbf{u}_s' = \overline{\int_{t_0}^{t} \mathbf{u}'(t')\,dt' \cdot \nabla \mathbf{u}'} \tag{14}$$

with a similar expression for the lower layer, where the overbar denotes an average over a

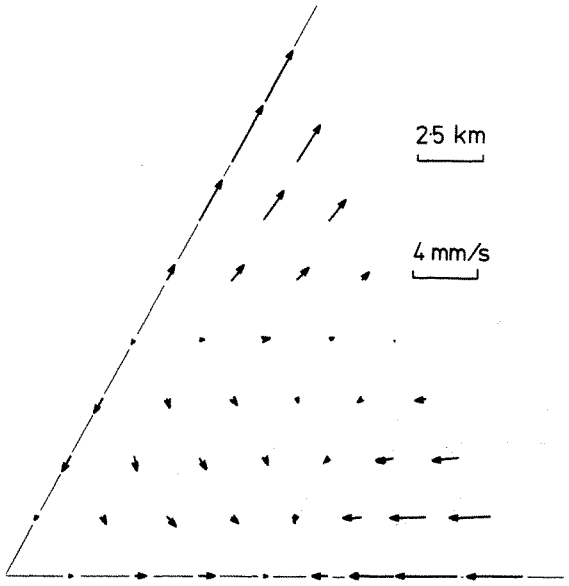

Figure 2. Stokes drift for the upper layer

complete tidal period. Using the complex notation of (11), we obtain

$$\mathbf{u}_s' = \frac{1}{2\sigma} \operatorname{Im} \left(\mathbf{U}_1 \cdot \nabla \mathbf{U}_1^* + \frac{h''}{h} (\mathbf{U}_1 \cdot \nabla \mathbf{U}_2^* + \mathbf{U}_2 \cdot \nabla \mathbf{U}_1^*) + \frac{h''^2}{h^2} \mathbf{U}_2 \cdot \nabla \mathbf{U}_2^* \right) \tag{15}$$

and

$$\mathbf{u}_s'' = \frac{1}{2\sigma} \operatorname{Im} \left(\mathbf{U}_1 \cdot \nabla \mathbf{U}_1^* - \frac{h'}{h} (\mathbf{U}_1 \cdot \nabla \mathbf{U}_2^* + \mathbf{U}_2 \cdot \nabla \mathbf{U}_1^*) + \frac{h'^2}{h^2} \mathbf{U}_2 \cdot \nabla \mathbf{U}_2^* \right). \tag{16}$$

Packham and Williams[6] obtained closed analytical solutions for the tidal Helmholtz equations (12) for a wedge-shaped estuary with angle $\pi/(2n+1)$, where n is an integer. Dyke[7]

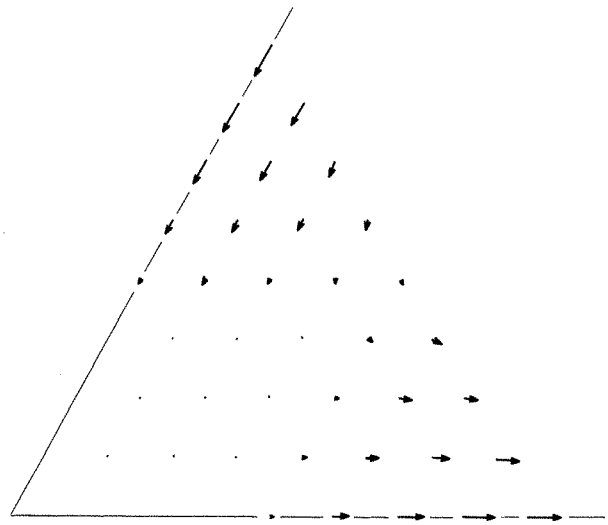

Figure 3. Stokes drift for the lower layer

calculated the Stokes drift for a two-layer estuary of wedge angle $\pi/3$. The Stokes drift field for both layers in this estuary is shown in Figures 2 and 3; the following values were used for the physical quantities:

$$\begin{aligned} &f = 1{\cdot}209\times10^{-4}\,\mathrm{s}^{-1}; \qquad \sigma = 1{\cdot}405\times10^{-4}\,\mathrm{s}^{-1}; \qquad \alpha = 0{\cdot}01 \\ &|Z_1| = 1{\cdot}918\ \mathrm{m\ at\ origin}; \qquad |Z_2| = 4{\cdot}666\times10^{-3}\ \mathrm{m\ at\ origin} \\ &g = 9{\cdot}81\ \mathrm{m\,s}^{-2}; \qquad h = 20\ \mathrm{m}; \qquad h' = 5\ \mathrm{m}; \qquad h'' = 15\ \mathrm{m} \end{aligned} \tag{17}$$

The choice of the relative magnitudes of $|Z_1|$ and $|Z_2|$ can be justified by requiring that the fractional change in layer thickness due to each mode is of the same magnitude.

3. NUMERICAL SOLUTION

Since real coastlines and bottom profiles have irregular shapes, it would be advantageous to choose a numerical method which can be used on an irregular mesh with, for example, greater resolution near the coast than out in the open sea. Various types of finite element method have been used successfully in engineering and other fields particularly for time independent problems and for sinusoidal oscillations, on such irregular meshes.

We therefore decide to see if a finite element method were suitable for this particular case. Because of the mixed nature of the coastal boundary condition, involving both normal and tangential derivatives, a variational finite element formulation is difficult. However, a Galerkin formulation is straightforward.

In order to build a Galerkin type finite element model, the Helmholtz tidal equation is written in the following weighted residual form:

$$\int_A (\nabla^2\zeta + k^2\zeta)\,\delta\zeta\,\mathrm{d}\mathbf{x} = 0 \tag{18}$$

where $\delta\zeta$ is an arbitrary functional variation of ζ. (The Z_m in (12) have been replaced by ζ and k_m by k).

Integrating by parts, we obtain

$$\int_A (-\nabla\zeta\,.\,\nabla\,\delta\zeta + k^2\zeta\,\delta\zeta)\,\mathrm{d}\mathbf{x} + \int_{\partial A} \frac{\partial\zeta}{\partial n}\,\delta\zeta\,\mathrm{d}s = 0 \tag{19}$$

where $\partial\zeta/\partial n$ is the outward normal derivative of ζ on the boundary ∂A of the domain A. ∂A is composed of the open boundary $\partial_1 A$, on which ζ is prescribed, and thus $\delta\zeta = 0$, and the coastal boundary $\partial_2 A$, on which the zero normal velocity condition requires

$$i\sigma\frac{\partial\zeta}{\partial n} + f\frac{\partial\zeta}{\partial s} = 0 \tag{20}$$

where s is directed anticlockwise around ∂A.

We thus have

$$\int_A (-\nabla\zeta\,.\,\nabla\,\delta\zeta + k^2\zeta\,\delta\zeta)\,\mathrm{d}\mathbf{x} - \frac{f}{i\sigma}\int_{\partial_2 A} \frac{\partial\zeta}{\partial s}\,\delta\zeta\,\mathrm{d}s = 0 \tag{21}$$

Now we expand ζ in terms of a number, N, of basis functions ϕ_j:

$$\zeta = \sum_{j=1}^{N} \phi_j\zeta_j \tag{22}$$

Since $\delta\zeta$ is an arbitrary small functional variation, (21) will be valid for $\delta\zeta = \varepsilon\phi_l$, $l = 1, 2, \ldots, N$, so

$$\sum_{j=1}^{N} M_{lj}\zeta_j = 0 \tag{23}$$

where

$$M_{lj} = \int_A (-\nabla\phi_l \cdot \nabla\phi_j + k^2\phi_l\phi_j)\,\mathrm{d}\mathbf{x} - \frac{f}{i\sigma}\int_{\partial_2 A} \phi_l \frac{\partial\phi_j}{\partial s}\,\mathrm{d}s \tag{24}$$

It can be seen from (13), (15) and (16) that in order for the Stokes drift to be evaluated sufficiently accurately, there must be sufficient accuracy in all the first and second derivatives of ζ. Linear basis functions over triangular elements are certainly not adequate, as the second derivatives are zero almost everywhere.

For a parallel sided canal, with boundary conditions giving rise to a single Kelvin wave solution of the form

$$\zeta = A \exp\frac{f}{c} y \exp i\left(\sigma t - \frac{\sigma}{c} x\right),$$

we found that quadratic basis functions over 6-noded triangular elements gave reasonable values for the elevation, but that the derivatives were inaccurate.[8] The second derivatives were less accurate than the first derivatives, and, being constant over each element, had marked discontinuities at the nodes, giving rise to ambiguities in evaluating terms such as $\mathbf{U}_1 \cdot \nabla\mathbf{U}_2^*$.

In principle, it is possible to use cubic basis functions, where the coefficients ζ_j are the values of ζ and its first derivatives at the vertices of each triangular element.[9] We found, however, that the first derivatives were still inaccurate, and there remained the problem of the discontinuous second derivatives.

For the above reasons we chose basis functions in which the coefficients ζ_j in (22) are the values of ζ and all its first and second derivatives (6 values in all) for each of the 45 nodes in the mesh of 64 triangular elements shown in Figure 4.

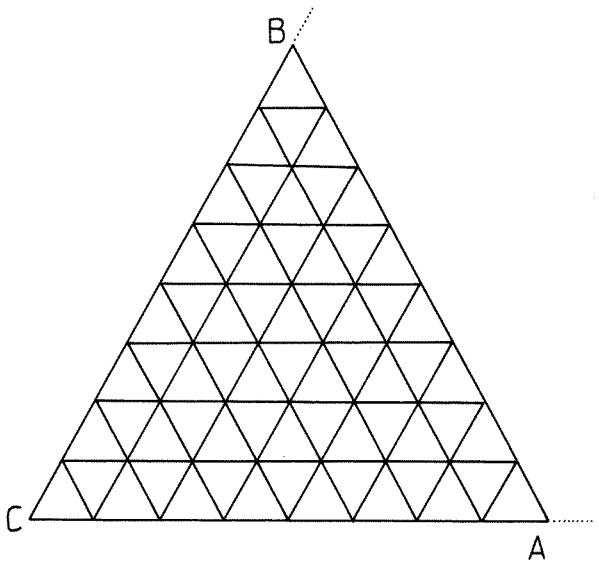

Figure 4. The 64-element triangular mesh. AB is the open boundary $\partial_1 A$. BCA is the coastal boundary $\partial_2 A$. Mesh size is 2·5 km

The basis functions used are the fifth degree, 18 parameter family of Hermite interpolation polynomials described by Mitchell and Wait (Reference 9, p. 74), amended where necessary to take account of the fact that the triangular elements are equilateral rather than right-angled and isosceles. [NB: Mitchell and Wait's basis function $\phi_2^{(0,0)}$ should be $p_2^2(10p_2 - 15p_2^2 + 6p_2^3 + 15p_1^2p_3)$.]

These basis functions give continuity of first derivatives everywhere, and continuity of second derivatives at the nodes. For the particular basis functions used, the triangular mesh must be derivable by a linear transformation (or a suitable non-linear transformation) from a mesh of isosceles right-angled triangles. If we are to use a mesh of arbitrary triangles, to approximate more closely the shape of a real estuary, basis functions similar to those used by Bell[10] must be used, the polynomial coefficients of which are evaluated by inversion of a 21×21 matrix for every element.

Numerical integration was used to evaluate the matrix elements M_{ij} for each triangular elements, and the elemental matrix elements were assembled (by summation) into a square global unsymmetric banded complex matrix of size

$$6 \times (\text{number of nodes}) \times [12 \times (\text{maximum difference between node numbers} + 1) - 1]$$

In order for the numerical integration to be exact, 36 point 11th degree Gaussian integration was used for the integrals over the triangular elements[11,12] and 5 point 9th degree Gaussian integration was used for the integrals along the coastal boundary segments.

For ζ to be specified sufficiently accurately along $\partial_1 A$, it is necessary to specify the nodal values not only of ζ but also of its first and second derivatives along the boundary. It is therefore necessary to apply appropriate rotational transformations to the matrix elements which involve the derivatives of ζ at the nodes on $\partial_1 A$. If the axes $(s, -n)$ can be obtained from (x, y) by an anticlockwise rotation of θ, then

$$\begin{bmatrix} \zeta \\ \dfrac{\partial \zeta}{\partial s} \\ -\dfrac{\partial \zeta}{\partial n} \\ -\dfrac{\partial^2 \zeta}{\partial s\, \partial n} \\ \dfrac{\partial^2 \zeta}{\partial s^2} \\ \dfrac{\partial^2 \zeta}{\partial n^2} \end{bmatrix} = \mathbf{R}^{-1} \begin{bmatrix} \zeta \\ \dfrac{\partial \zeta}{\partial x} \\ \dfrac{\partial \zeta}{\partial y} \\ \dfrac{\partial^2 \zeta}{\partial x\, \partial y} \\ \dfrac{\partial^2 \zeta}{\partial x^2} \\ \dfrac{\partial^2 \zeta}{\partial y^2} \end{bmatrix} \tag{25}$$

where

$$\boldsymbol{R} = \begin{bmatrix} 1 & 0 & 0 & 0 & 0 & 0 \\ 0 & C & -S & 0 & 0 & 0 \\ 0 & S & C & 0 & 0 & 0 \\ 0 & 0 & 0 & C^2 - S^2 & CS & -CS \\ 0 & 0 & 0 & -2CS & C^2 & S^2 \\ 0 & 0 & 0 & 2CS & S^2 & C^2 \end{bmatrix} \tag{26}$$

with $C = \cos\theta$ and $S = \sin\theta$.

The appropriate transformations to be applied to the global matrix, for node l on $\partial_1 A$ are

$$\mathbf{M}_{jl}^{s\prime} = \mathbf{M}_{jl}^{s}\mathbf{R},\ j = 1, \ldots l-1, l+1, \ldots, \frac{N}{6}$$

$$\mathbf{M}_{lj}^{s\prime} = \mathbf{R}^T\mathbf{M}_{lj}^{s},\ j = 1, \ldots l-1, l+1, \ldots, \frac{N}{6} \tag{27}$$

and

$$\mathbf{M}_{ll}^{s\prime} = \mathbf{R}^T\mathbf{M}_{ll}^{s}\mathbf{R}$$

where $\mathbf{M}_{lj}^{s}$ is the 6×6 submatrix relating node l to node j.

Once the rotations have been performed for all nodes on $\partial_1 A$, the prescribed values of ζ and its first and second tangential derivatives are set as described by Connor and Brebbia (Reference 13, p. 78). Their method sets all the matrix elements involving the prescribed values to zero except the diagonal element which is set to 1, and makes appropriate adjustments to a column vector, which we shall call $\mathbf{P}$, which is initially set to zero to represent the RHS of (23).

The system of linear equations can now be represented as

$$\sum_{j=1}^{N} M'_{lj}\zeta'_j = P_l \tag{28}$$

which is solved for the unknown ζ'_l by a method of Gaussian elimination similar to that described by Connor and Brebbia (Reference 13, p. 83). The inverse transformation to (25) then performed for all the nodes on $\partial_1 A$, and the nodal values of $\mathbf{U}$ and $\nabla\mathbf{U}$ are obtained by applying (13) to the nodal values of the first and second derivatives of ζ. The Stokes drift at each node can then be obtained by applying (15) and (16).

The above method was used to determine the Stokes drift field for the two-layer wedge shaped estuary of angle $\pi/3$ with physical quantities as specified in (17). The values of ζ and its tangential derivatives on the open boundary $\partial_1 A$ were introduced into the rotated system of linear equations (28) as described above.

The length of the sides of the elements for the 64-element mesh is approximately $\frac{1}{10}$ of the wavelength $2\pi c_2/\sigma$ of a Kelvin wave solution for mode 2.

We found that the 64-element mesh produced a satisfactory solution for mode 2, but the longer wavelength mode 1 developed numerical errors which reduced the accuracy of the velocity and its derivatives to an unacceptable extent, giving rise to inaccuracies of up to 20 per cent in the resulting Stokes drift.

These errors may be due to rounding, since we are using the second spatial derivatives of a mode with a very long wavelength—in order of magnitude terms, where Δx is the mesh size (2·5 km),

$$\left(\Delta x^2 \frac{\partial^2 Z_1}{\partial x^2}\right)/Z_1 \sim 2\times 10^{-4} \tag{29}$$

The accuracy to which the node co-ordinates and boundary conditions were given was 6–7 significant figures ($\sim 10^{-6}$), which, in computational terms, is not negligible compared with the above parameter. For more realistic physical problems with irregular coastlines and frictional effects, the node 1 derivatives will increase markedly, with parameter (29) increasing correspondingly, so we would not expect rounding to give rise to such large errors.

In fact, the numerical errors were eliminated when the equation for mode 1 was solved on a 16-element mesh and the values of the mode 1 variables at the intermediate points were obtained by interpolation, using the basis functions as interpolation functions.

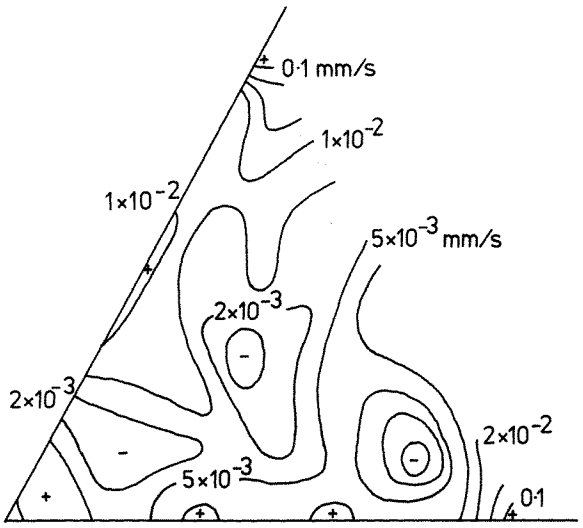

Figure 5. Error in finite-element calculation of Stokes drift, for the upper layer

The Stokes drift field for the above finite-element solution is in satisfactory agreement with the analytical result shown in Figures 2 and 3: the errors are shown in Figures 5 and 6. It can be seen that the maximum errors (about 5 per cent) occur at the nodes at either end of the open boundary.

The finite-element program was written in a version of Fortran IV and was run on the Aberdeen University Honeywell Level 66 computer. It took $3\frac{1}{2}$ minutes to run, using 86k words of core storage. Neither the matrix assembly process not the Gaussian elimination process was optimized: optimization would lead to a significant reduction in run-time.

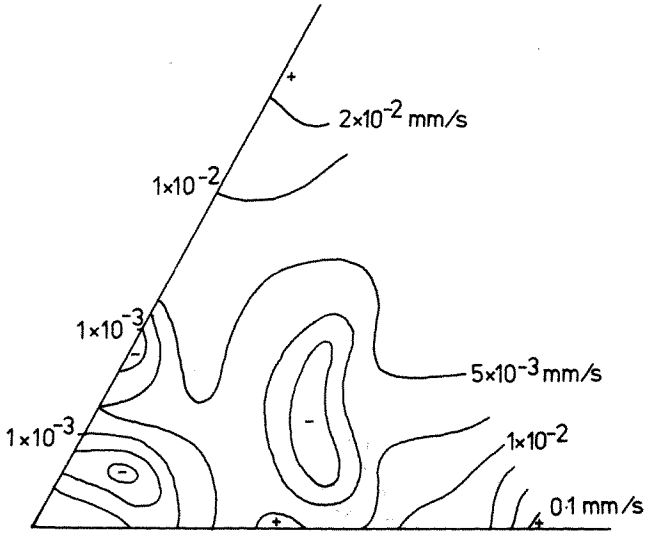

Figure 6. Error in finite element calculation of Stokes drift, for the lower layer

The same finite element method was also used to solve the linearized tidal equations in a rectangular basin.[8] Good agreement was obtained with G. I. Taylor's solution of the problem.[14]

It should be possible to verify the numerical method in the laboratory, using salt solutions of varying density, with the apparatus mounted on a rotating turntable. Field verification should also be possible, once the model is developed further, to include the effects of variable depth and friction. Suitable measurements of currents, preferably including some Lagrangian techniques such as drogues or dye tracers, would need to be made in a stratified estuary or other region, preferably deep enough for the tidal motions to be approximately linear.

4. CONCLUSION

It can be seen from the previous section that a fifth-degree finite element method, using triangular elements similar to each other, with sides about $\frac{1}{10}$ of the wavelength of a Kelvin wave solution for the interfacial mode, provides reasonably accurate values for the Stokes drift in a wedge-shaped two-layer estuary of constant depth with zero bottom friction. By making suitable alterations to the finite element method, it should be possible to use triangular elements of arbitrary shape, and thus determine Stokes drift fields for estuaries with more general shapes.

ACKNOWLEDGEMENTS

The author is in receipt of a Research Associateship provided by funds from the U.K. Science Research Council under the Marine Technology programme. The derivation of (21) was suggested by Dr. R. Wait.

REFERENCES

1. M. S. Longuet-Higgins, 'On the transport of mass by time-varying ocean currents', *Deep-Sea Research*, **16,** 431–447 (1969).
2. P. P. G. Dyke, 'Steady flows induced by tidal oscillations in coastal waters', *Ph.D. Thesis*, University of Reading, 1972.
3. H. D. Dooley, 'A comparison of drogue and current meter measurements in shallow waters, *Rapp. P.-v. Réun. Cons. int. Explor. Mer*, **167,** 225–230 (1974).
4. P. P. G. Dyke, 'On the Stokes' drift induced by tidal motions in a wide estuary', *Estuarine and Coastal Marine Science*, **11,** 17–25 (1980).
5. M. Rattray Jr., 'Time-dependent motion in an ocean; a unified two-layer, beta-plane approximation', *Studies on Oceanography*, 19–29 (1964).
6. B. A. Packham and W. E. Williams, 'The diffraction of Kelvin waves at a corner', *J. Fluid Mechanics*, **34,** 517–529 (1968).
7. P. P. G. Dyke, 'Residual currents in a wide estuary—a mathematical model', *Proceedings of the European Conference on Environmental Pollution*, Frankfurt, 17th–19th December 1980.
8. A. D. Jenkins, 'Determination of tidal residual currents in wide estuaries, using finite element methods', in C. Taylor and B. A. Schrefler (eds.), *Numerical Methods in Laminar and Turbulent Flow*, Pineridge Press, Swansea, UK, 1981, pp. 753–762.
9. A. R. Mitchell and R. Wait, *The Finite Element Method in Partial Differential Equations*, Wiley, London, 1977.
10. K. Bell, 'A refined triangular plate-bending finite element', *Int. J. Num. Meth. Eng*, **1,** 101–122 (1969).
11. P. C. Hammer, O. J. Marlowe and A. H. Stroud, 'Numerical integration over simplexes and cones', *Math. Tables and Other Aids to Computation*, **10,** 130–136 (1956).
12. H. Fishman, 'Numerical integration constants', *Math. Tables and Other Aids to Computation*, **11,** 1–9 (1957).
13. J. J. Connor and C. A. Brebbia, *Finite Element Techniques for Fluid Flow*, Butterworths, London, 1977.
14. G. I. Taylor, 'Tidal oscillations in gulfs and rectangular basins', *Proc. Lond. Math. Soc.*, **20,** 148–181 (1920).